

# Validation of inferred high resolution ocean pCO<sub>2</sub> and air-sea fluxes with in-situ and remote sensing data.

Ismael Hernandez, Hussein Yahia, Joël Sudre, Véronique Garçon, Christoph Garbe, Boris Dewitte, Séréna Illig, Ivonne Montes, Aurélien Paulmier, André Butz

LEGOS, Toulouse, France  
University of Heidelberg, Germany  
Géostat, INRIA, Bordeaux  
Karlsruhe Institute for Technology, Germany

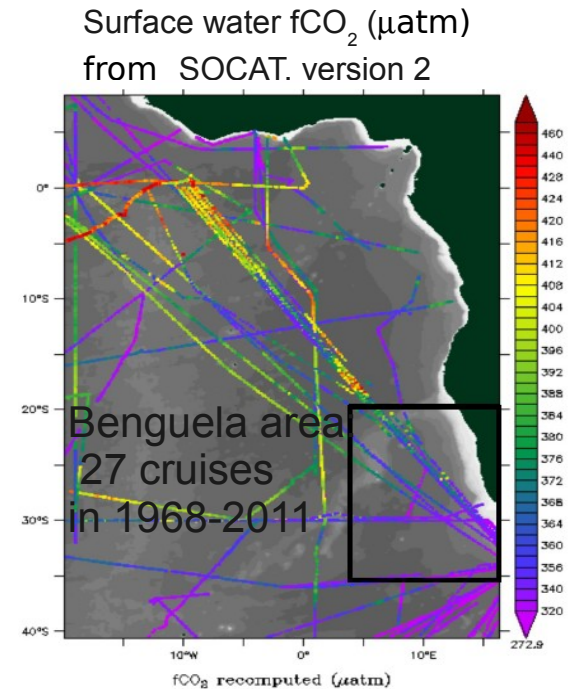
**STSE ESA OceanFlux - Theme 3 : Upwelling**



**oceanflux**  
support to science element

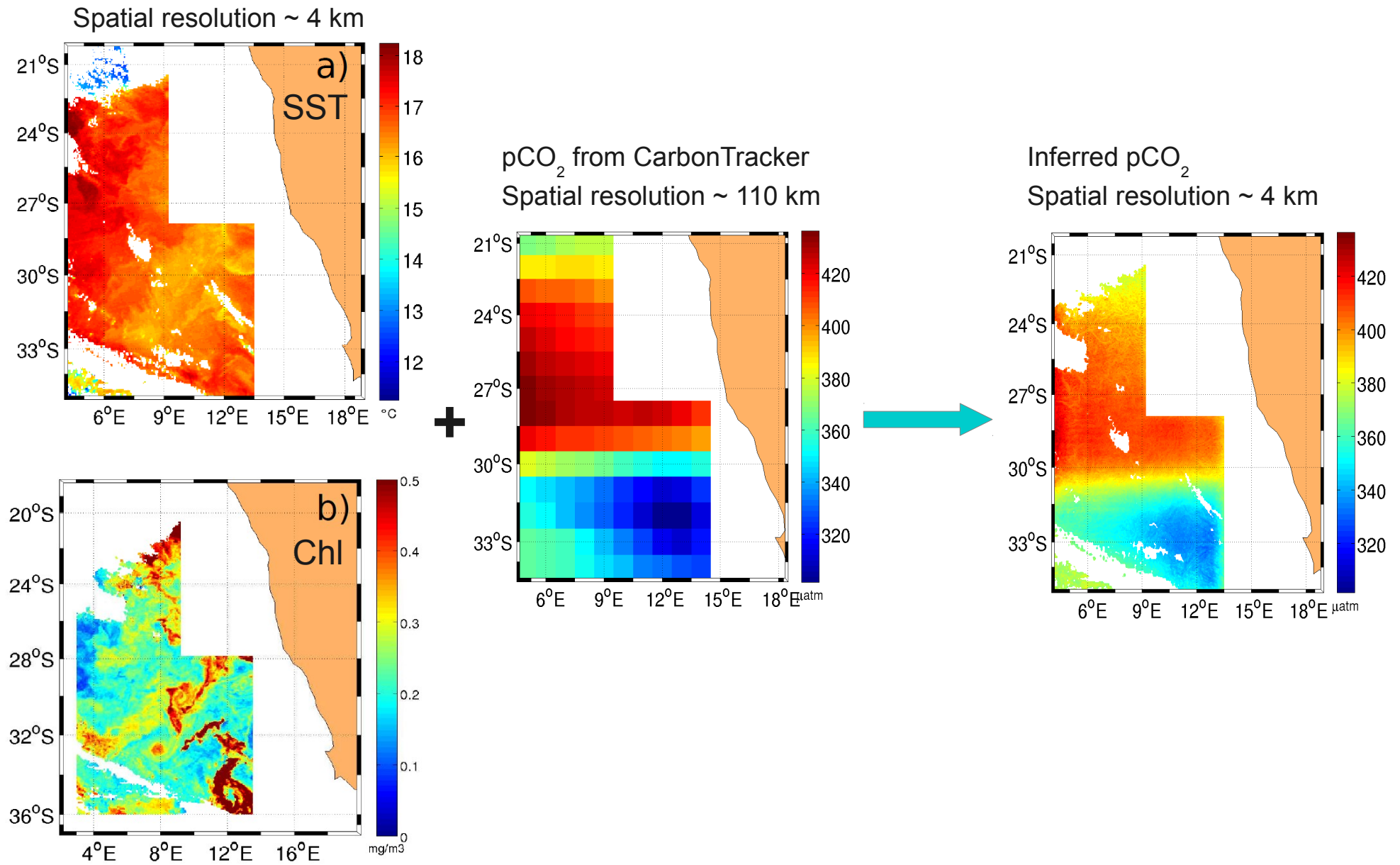
# Why this work?

- Importance of submesoscale features.
- Scarcity of oceanographic cruises and lack of available satellite products.



- GOAL: To obtain an assesment of spatial variability of GHGs concentrations at small scales ( $\sim 4$  km) from satellite images in the EBUS.

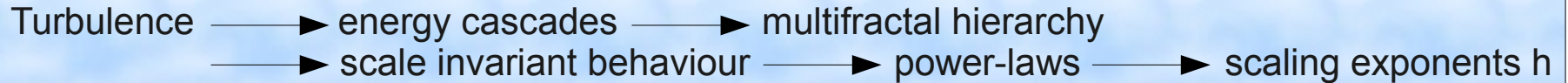
# The idea



Variations in phytoplankton (carbon cycling), Variations in temperature (solubility) → Variations in CO<sub>2</sub>

# How to do it?

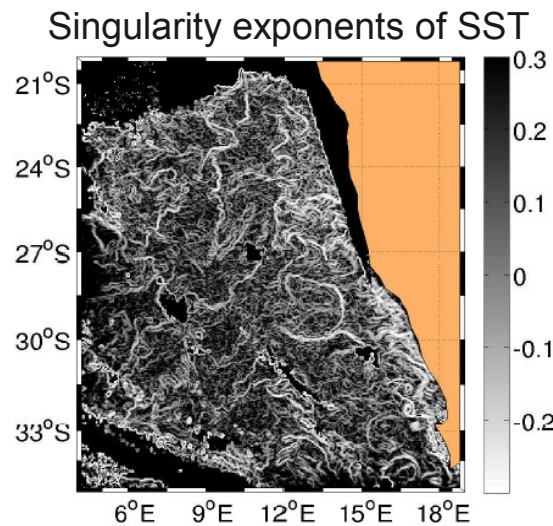
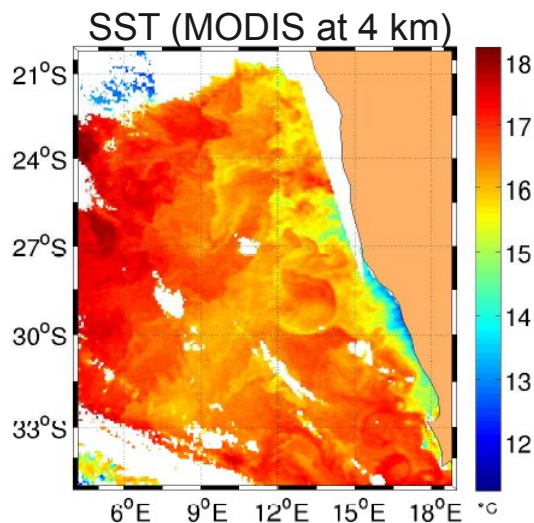
## 1. How to obtain the small scale information?



Microcanonical Multiscale Formalism:  
Set of scaling exponents obtained as sets of geometrically localized singularity exponents.

$$\mathcal{F}_h = \{\mathbf{x} : h(\mathbf{x}) = h\}$$

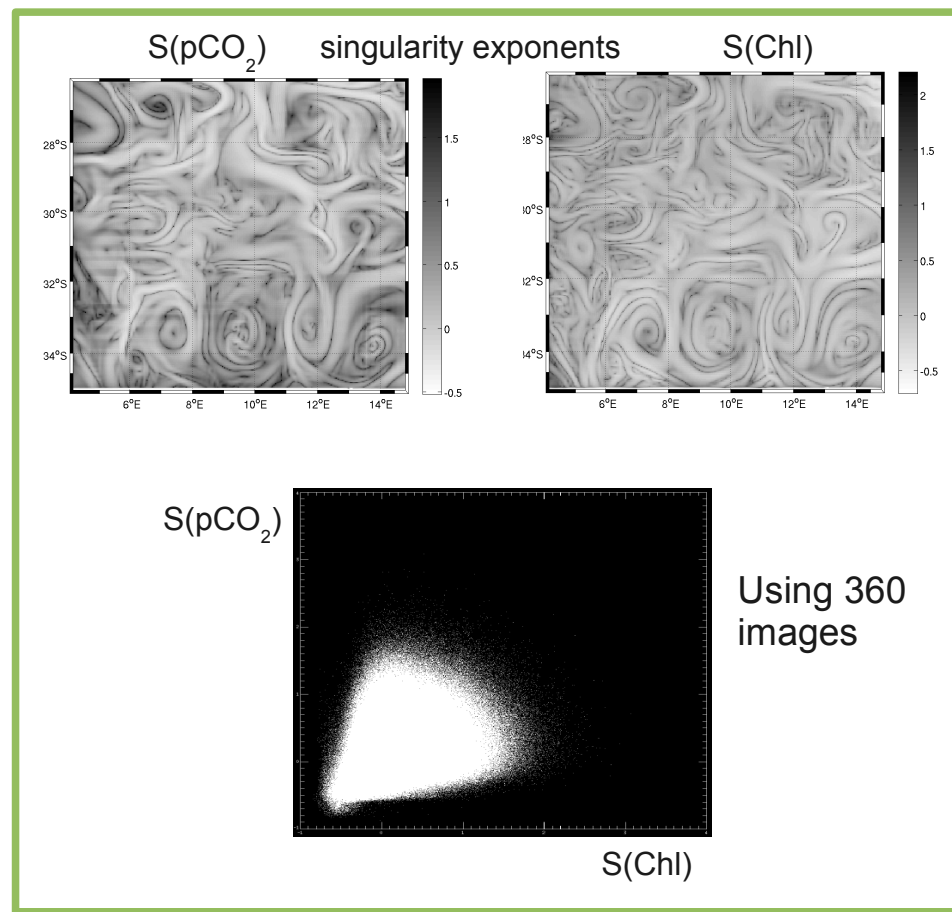
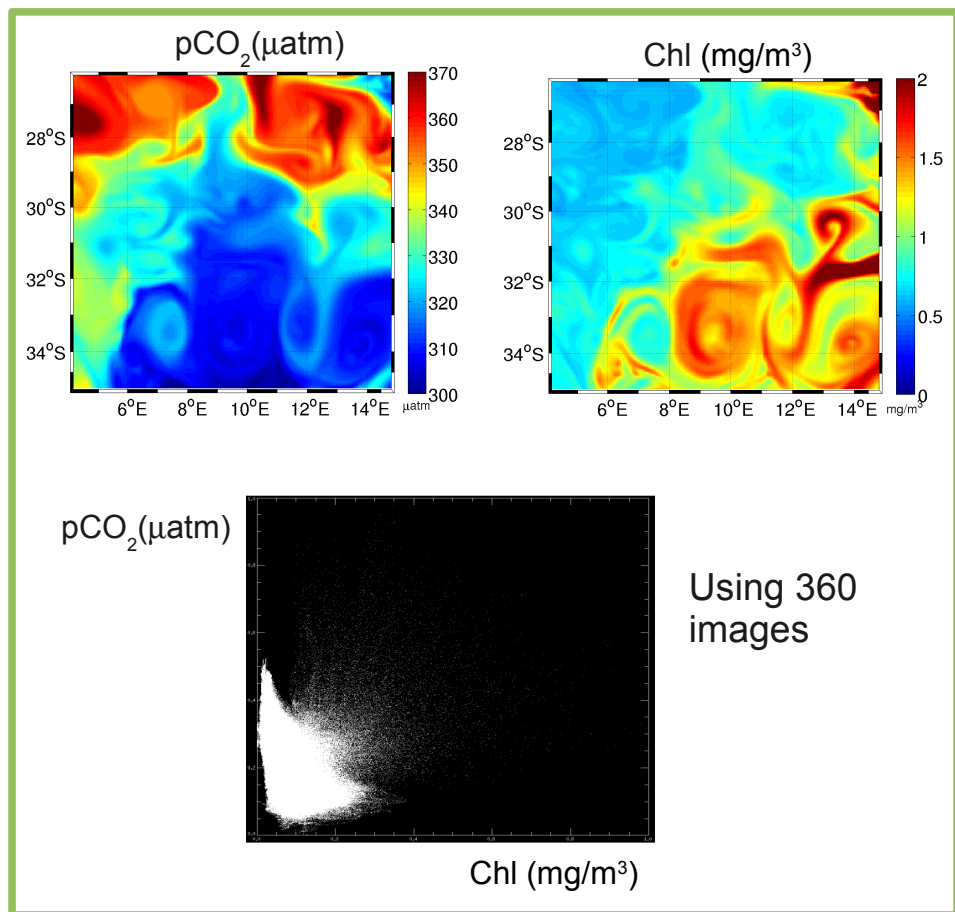
$$\left. \begin{aligned} \frac{1}{r} |s(\mathbf{x} + \mathbf{r}) - s(\mathbf{x})| &\sim r^{h(\mathbf{x})} \\ \mathcal{T}_\psi |\nabla s|(\mathbf{x}, r) &= \alpha(\mathbf{x}) r^{h(\mathbf{x})+d} + o(r^{h(\mathbf{x})+d}) \quad (r \rightarrow 0) \end{aligned} \right\} h(x) = \frac{\log(\mathcal{T}_\psi |\nabla s|(\mathbf{x}, r_0) / \langle \mathcal{T}_\psi |\nabla s|(\cdot, r_0) \rangle)}{\log r_0} + o\left(\frac{1}{\log r_0}\right)$$



- Measure of the degree of regularity of the image, associated to transitions

## 2. How to connect different tracer images?

ROMS-BIOEBUS model in the Benguela upwelling system



$$pCO_2 \neq pCO_2(SST, CHL)$$

$$S(pCO_2) = S(pCO_2)(S(SST), S(CHL))$$

Proxy of  
S(pCO<sub>2</sub>)  
at high  
resolution:

$$S(pCO_2)(\mathbf{x}) = a(\mathbf{x})S(SST)(\mathbf{x}) + b(\mathbf{x})S(Chl - a)(\mathbf{x}) + c(\mathbf{x})S(pCO_2^{LR})(\mathbf{x}) + d(\mathbf{x})$$

Regression coefficients  $a(x), b(x), c(x), d(x)$  are estimated from ROMS-BIOEBUS output data

### 3. Cross-scale inference of pCO<sub>2</sub> data

Multiresolution analysis on signal  $S(\text{pCO}_2)$  (proxy of pCO<sub>2</sub> at high resolution)

Decomposition of the signal at different scales: Wavelet projections

$$\mathcal{T}_\psi \mathcal{S}(\text{pCO}_2)(\mathbf{x}, \mathbf{r}_j) = \sum_{n \in \mathbb{Z}} \langle \mathcal{S}(\text{pCO}_2) | \psi_{x_n, r_j} \rangle \psi_{x_n, r_j}(u)$$

$\mathbf{A}_j$  orthogonal projection of  $\mathbf{V}_j$  (approximation space)

$\mathbf{P}_j$  orthogonal projection of  $\mathbf{W}_j$  (detail space)



Reconstruction formula:

$$A_{j-1} \text{pCO}_2 = A_j \text{pCO}_2 + P_j h$$



# Input Data

- CarbonTracker air-sea fluxes at low resolution:  $1^\circ \sim 110$  km

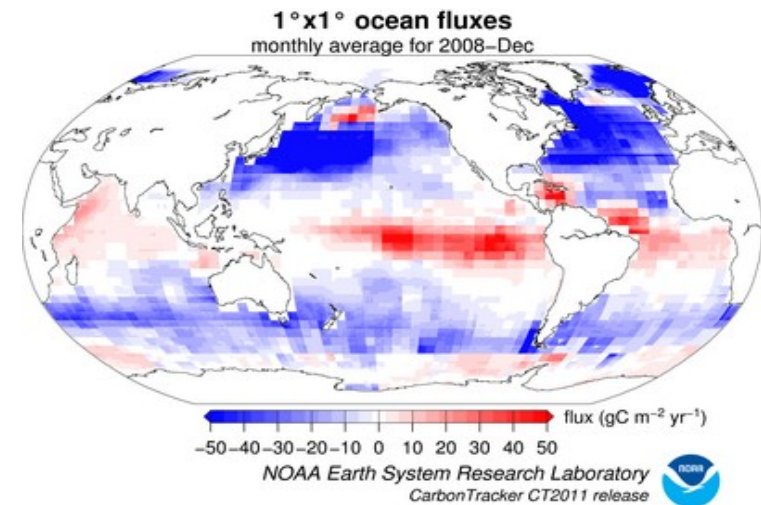
Temporal evolution of a tracer  $c$  in the atmosphere :

$$\frac{\partial c}{\partial t} = -u\nabla c + \frac{1}{\rho}\nabla(\rho T_d \nabla c) + \frac{1}{\rho}g + \mathbf{F}$$

$F$ , net flux at the interface

Atmospheric  $\text{CO}_2$  data provided by SCIAMACHY and GOSAT. (Garbe *et al.* 2007, 2014)

Air-sea  $\text{CO}_2$  fluxes from CarbonTracker ( $1^\circ \times 1^\circ$  spatial resolution)  
(Peters *et al.* 2007)



Relation between net air-sea flux and  $p\text{CO}_2$

$$\mathbf{F} = \alpha K (p_{\text{CO}_2}^{\text{air}} - p_{\text{CO}_2}^{\text{ocean}})$$

- $p_{\text{CO}_2}^{\text{ocean}}$  obtained from inverse modeling and satellite data at resolution of CarbonTracker .

# Input Data

- SST and Chl-a from Satellite at high resolution: ~ 4 km

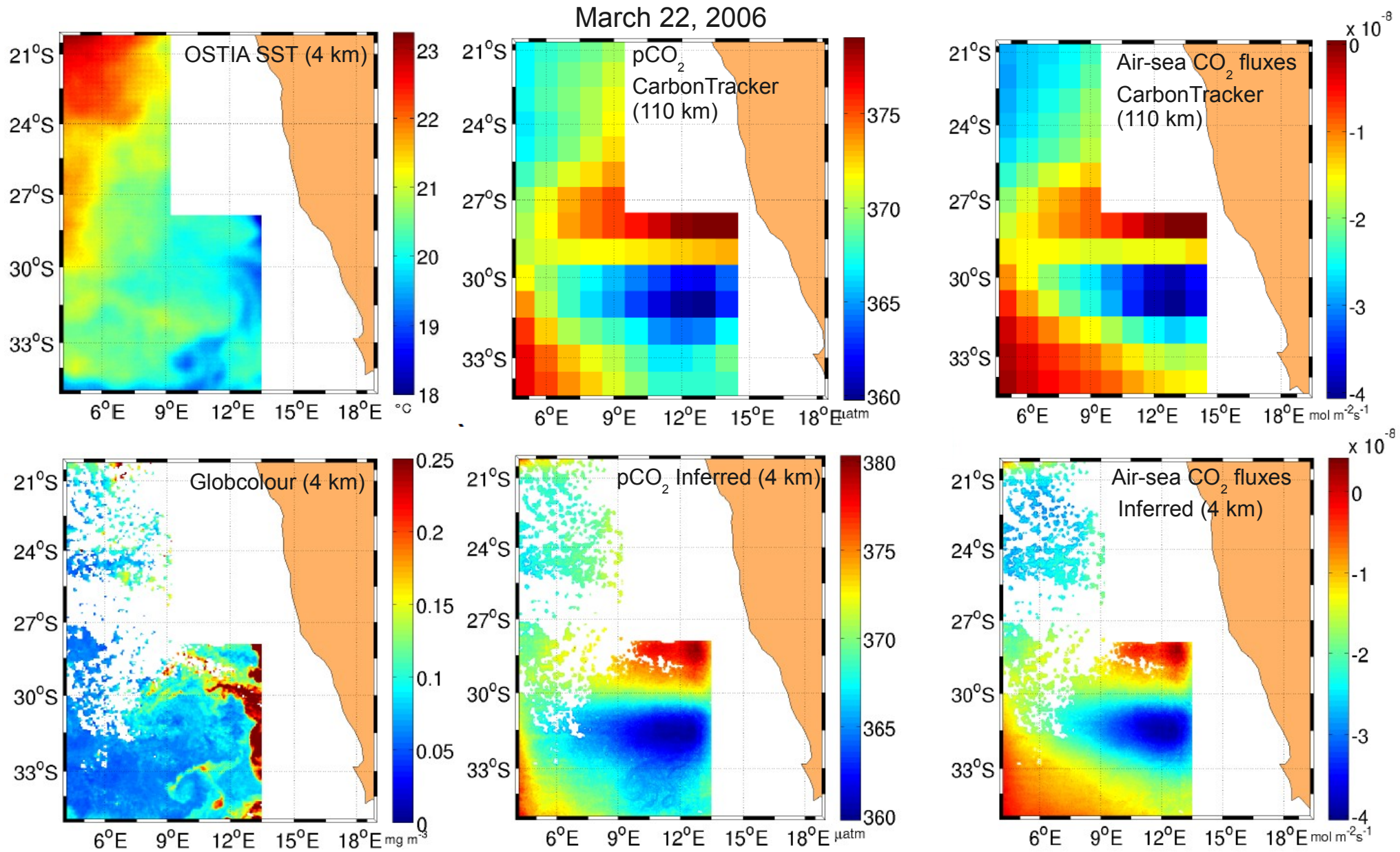
Name reference	Parameter	Instruments	Satellites	Resolution
OSTIA	SST	Optimal interpolation		5 km / daily
MODIS	SST	MODIS	AQUA	4 km / daily
MERIS	Chl-a	MERIS	ENVISAT	4 km / daily
Globcolour	Chl-a	MODIS/MERIS/SeaWiFS (Merged globcolour)	AQUA/ENVISAT	4 km / daily

Three combinations of Chl-a and SST products:

- MERIS-OSTIA
- Globcolour-OSTIA
- Globcolour-MODIS



# Super-resolution pCO<sub>2</sub> in the Benguela Upwelling System

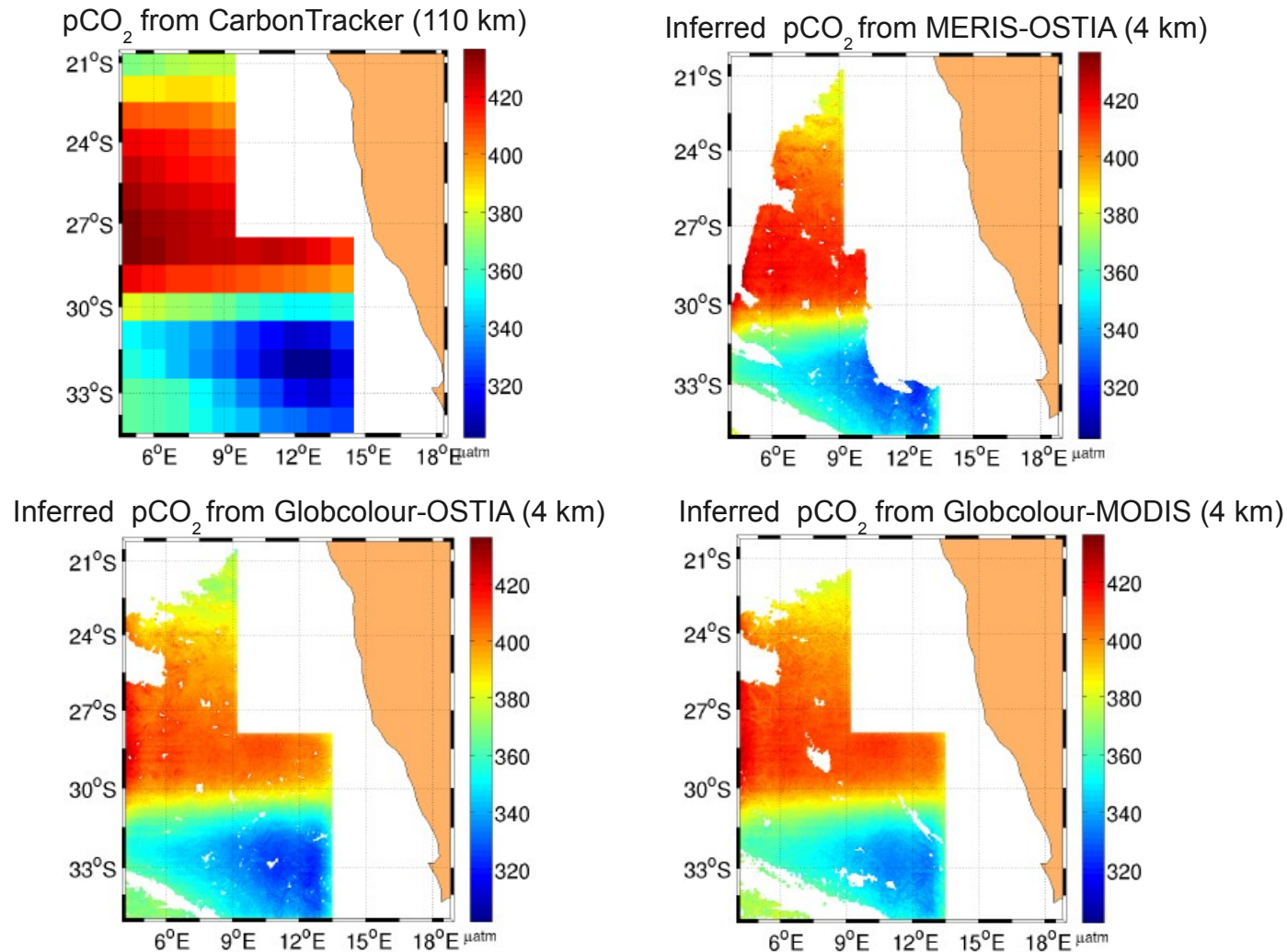


The cascade of information across the scales enhances gradients in the field of pCO<sub>2</sub>

# Evaluation analysis of using different satellite data combinations:

- Number of valid points yielded in the inferred  $p\text{CO}_2$  field
- Degradation of the information contained in the transition fronts

Septembre 21, 2006



**- Number of valid points yielded in the inferred pCO<sub>2</sub> field**

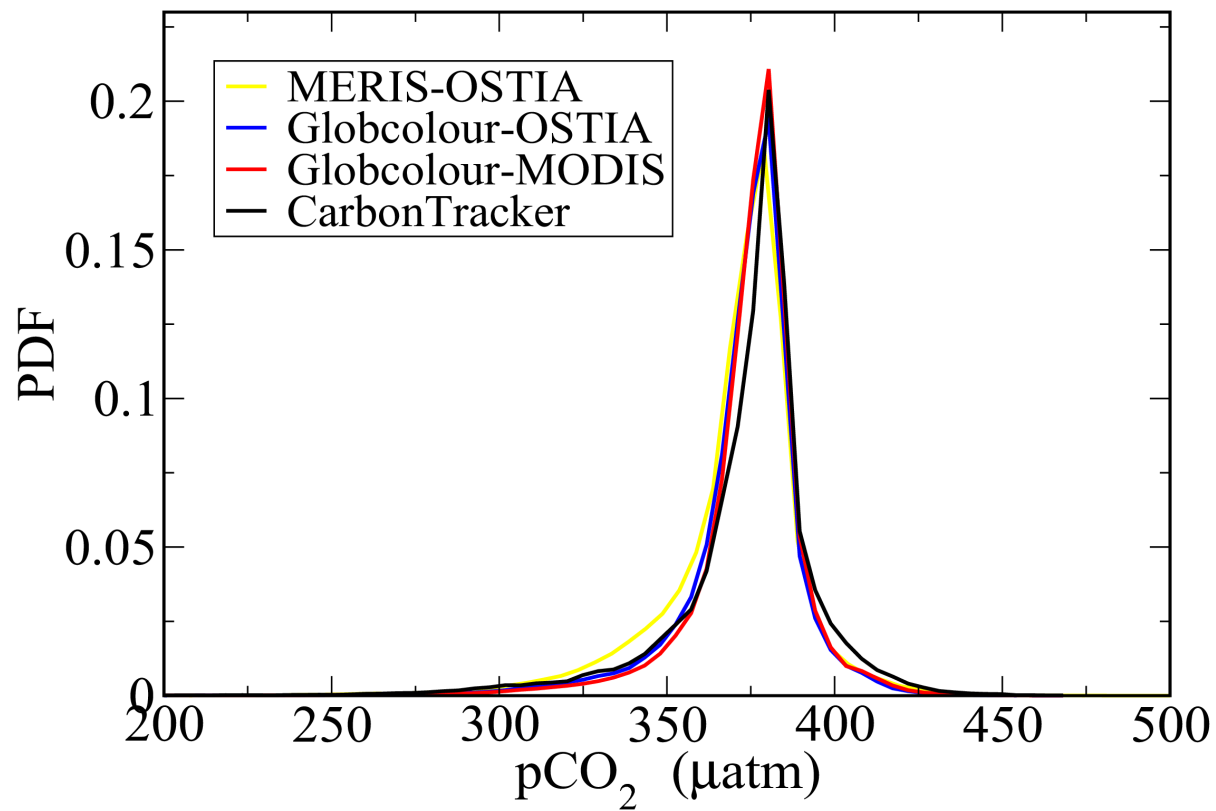
Valid Points in the inferred pCO <sub>2</sub> fields: 2006/2008	
N° total pixels domain	55711378
N° Points OSTIA-MERIS	9800776
N° Points OSTIA-GLOBCOLOUR(AVW)	26382072
N° Points OSTIA-GLOBCOLOUR(GSM)	27313043
N° Points MODIS-GLOBCOLOUR(GSM)	20397047
Proportion OSTIA-GSM/OSTIA-MERIS	2.78
Proportion OSTIA-GSM/MODIS-GSM	1.33
Proportion MODIS-GSM-/OSTIA-MERIS	1.08
$LP_{OM}$	82%
$LP_{OG}(AVW)$	53%
$LP_{OG}(GSM)$	51%
$LP_{MG}$	63%

- loss of valid points: 
$$LP_x = \frac{N_p - N_x}{N_p} 100\%$$

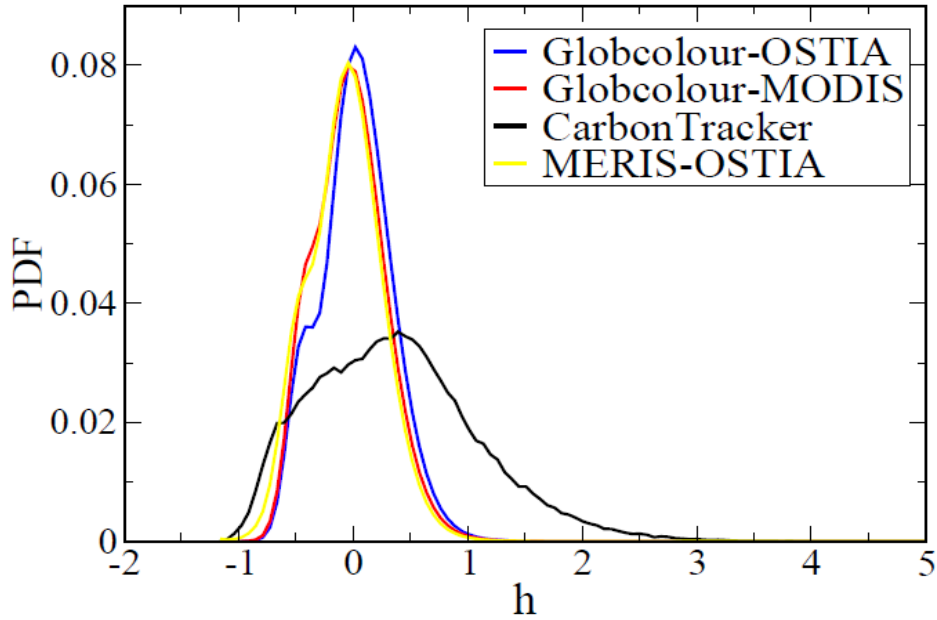
$N_p$  = 557711378, total number of pixels removing the pixels of the CarbonTracker mask  
 $N_x$  = number of valid points in the inferred pCO<sub>2</sub> for each product combination.

# Analysis of degradation of the realism of the transition fronts

- analysis of probability distribution functions (PDFs) of pCO<sub>2</sub> values



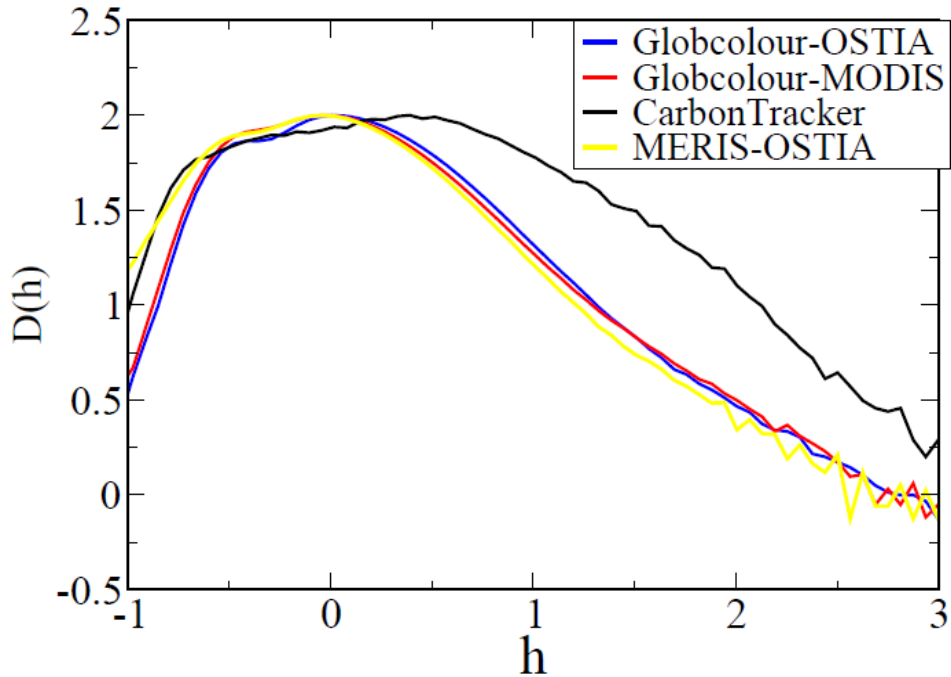
## - analysis of PDFs of singularity exponents of pCO2



- Scale dependent of PDFs
- Multifractal character

$$\rho_{r_0}(h) = A_0 r_0^{d-D(h)}$$

## - analysis of singularity spectra



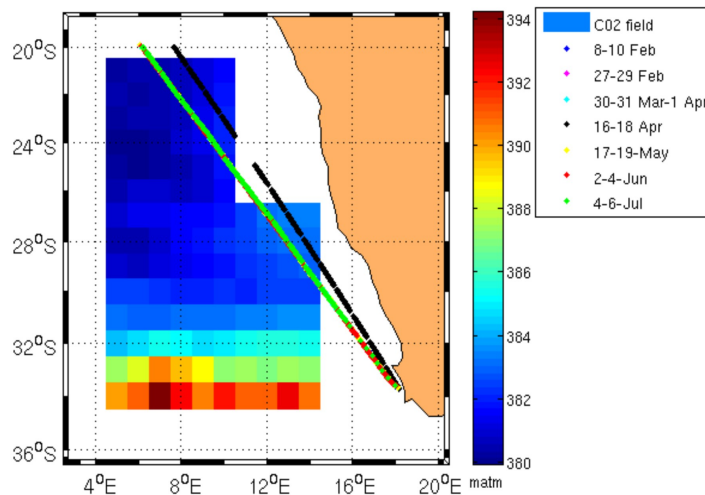
$$D(h) = d - \frac{\log(\rho_{r_0}(h)/\rho_{r_0}^M)}{\log r_0} \quad \rho_{r_0}^M = \max_h \{\rho_{r_0}(h)\}$$



# Validation with in-situ measurements

Available cruise data from SOCAT (Surface Ocean CO<sub>2</sub> Atlas) in the Benguela upwelling region

- 2000, one cruise: *ANT-18-1*
- 2004, one cruise: *0404SFC-PRT*
- 2005, five cruises: *QUIMA2005-0804*, *QUIMA2005-0821*, *QUIMA2005-0922*, *QUIMA2005-1202*, *QUIMA2005-1220*
- 2006, eight cruises: *QUIMA2006-0326*, *QUIMA2006-0426*, *QUIMA2006-0514*, *QUIMA2006-0803*, *QUIMA2006-0821*, *QUIMA2006-0921*, *QUIMA2006-1013*, *QUIMA2006-1124*
- 2008, seven cruises: *QUIMAVOS2008-1*, *QUIMAVOS2008-2*, *QUIMAVOS2008-3*, *QUIMAVOS2008-4*, *QUIMAVOS2008-5*, *QUIMAVOS2008-6*, *QUIMAVOS2008-7*
- 2010, one cruise: *ANT27-1*

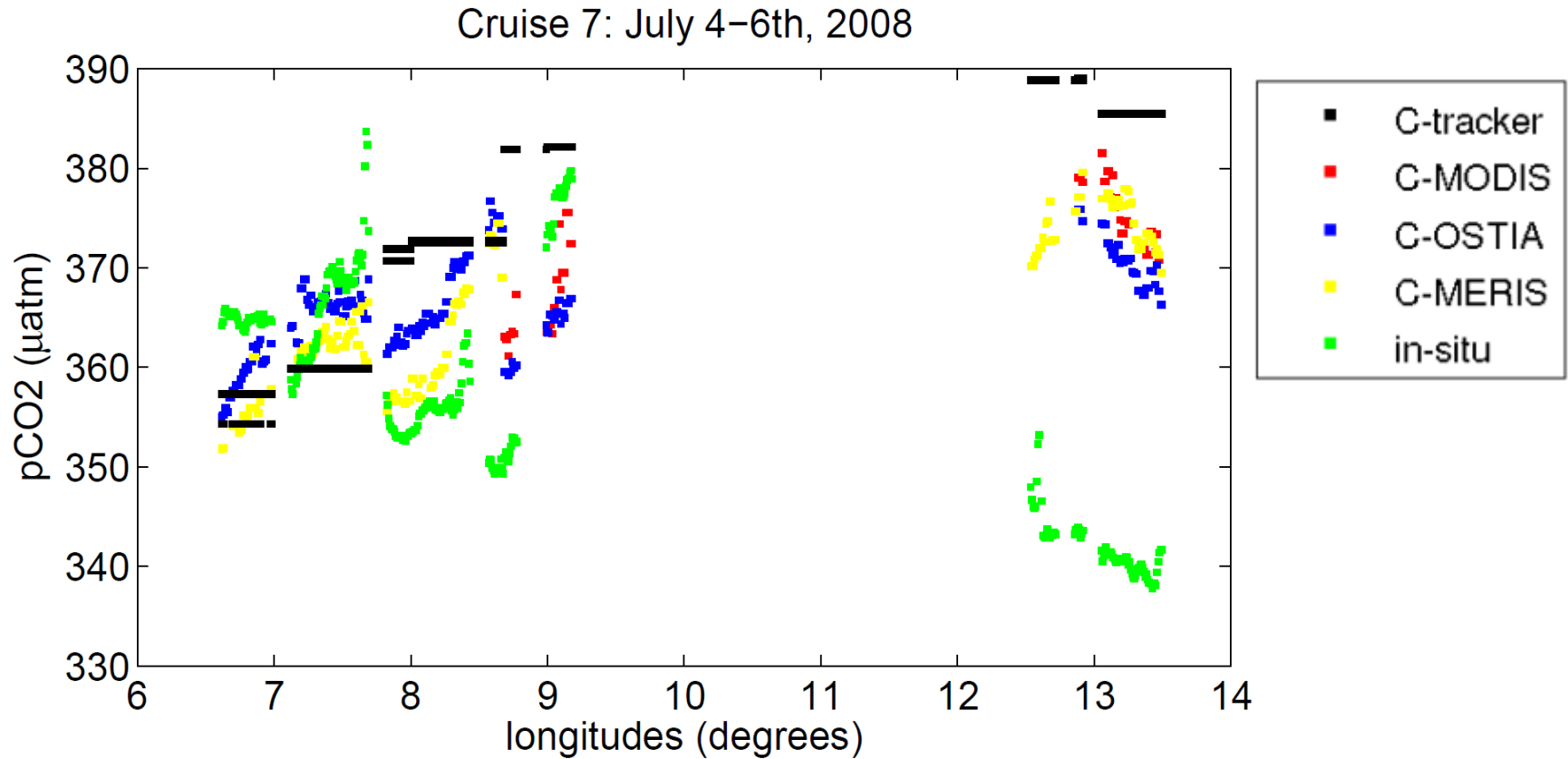


24 cruises in 2000-2010

We use QUIMA cruises in  
2005, 2006, 2008  
(20 cruises)



# Values of pCO<sub>2</sub> at the intersections: inferred field - in-situ measurement



Inferred pCO<sub>2</sub> values show small scale variability in the zonal direction

At all valid intersections points in each SST-OC combination

Statistical computations QUIMAVOS2006/2008			
	MERIS - OSTIA	Globcolour - OSTIA	Globcolour - MODIS
Number of valid intersections	747	1928	1460
Mean Error carbontracker-insitu ( $\mu atm$ )	2.97	8.83	14.93
Mean Error inferred-insitu ( $\mu atm$ )	-0.15	3.42	8.42
Mean Absolute Error carbontracker-insitu ( $\mu atm$ )	21.34	22.08	22.07
Mean Absolute Error inferred-insitu ( $\mu atm$ )	17.77	16.47	16.62
Mean Relative Error carbontracker-insitu	0.059	0.060	0.061
Mean Relative Error inferred-insitu	0.048	0.045	0.046

At the same valid intersections points in the three SST-OC combinations

Statistical computations QUIMAVOS2006-2008			
	MERIS - OSTIA	Globcolour - OSTIA	Globcolour - MODIS
Number of valid intersections	458	458	458
Mean Error carbontracker-insitu ( $\mu atm$ )	7.60	8.01	8.01
Mean Error inferred-insitu ( $\mu atm$ )	4.37	1.62	3.32
Mean Absolute Error carbontracker-insitu ( $\mu atm$ )	23.63	23.23	23.23
Mean Absolute Error inferred-insitu ( $\mu atm$ )	19.92	16.31	18.85
Mean Relative Error carbontracker-insitu	0.065	0.065	0.064
Mean Relative Error inferred-insitu	0.055	0.045	0.051

# Summing-up

- Novel method to reconstruct maps of ocean CO<sub>2</sub> fluxes at super resolution (~4km) from CarbonTracker CO<sub>2</sub> fluxes data at low resolution (~110 km).
- Inferred representation of pCO<sub>2</sub> improves the description provided by CarbonTracker.
- Merged products (Globcolour) improve the number of valid points in the pCO<sub>2</sub> field and the number of intersections for validation.
- Transitions fronts are well represented in the inferred pCO<sub>2</sub> using merged products.
- Mean absolute error with respect to *in-situ* measurements is smaller for the inferred pCO<sub>2</sub> than for CarbonTracker (16.3 and 23.2 μatm, respectively).

# What's the next

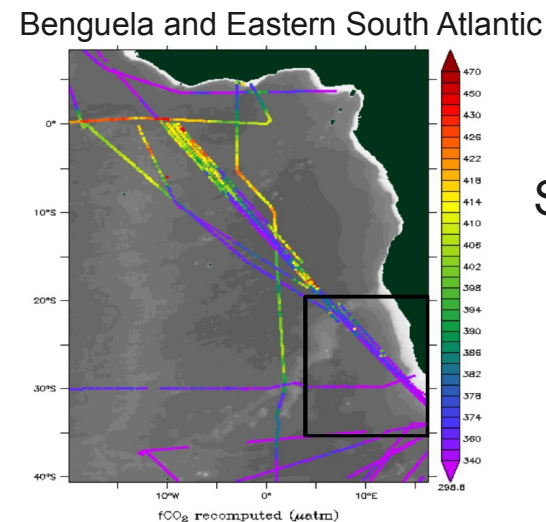
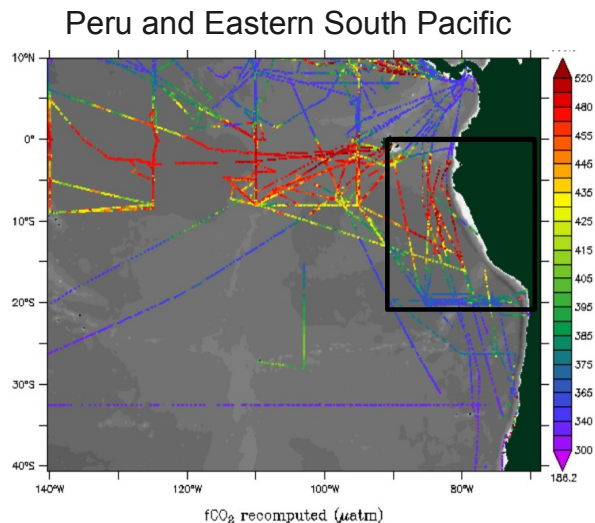
- Introduce seasonal and coefficients  $a(x)$ ,  $b(x)$ ,  $c(x)$  and  $d(x)$  of the multiple linear regression computed with a ROMS/BIOEBUS simulation.

$$\mathcal{S}(pCO_2^{ocean})(x) = a(x)\mathcal{S}(SST)(x) + b(x)\mathcal{S}(Chl\_a)(x) + c(x)\mathcal{S}(pCO_{2LR}^{ocean}) + d(x)$$

- Add the salinity parameter (Level 3 SMOS) in the inference of  $pCO_2$  as a new parameter in the multiple linear regression analysis.

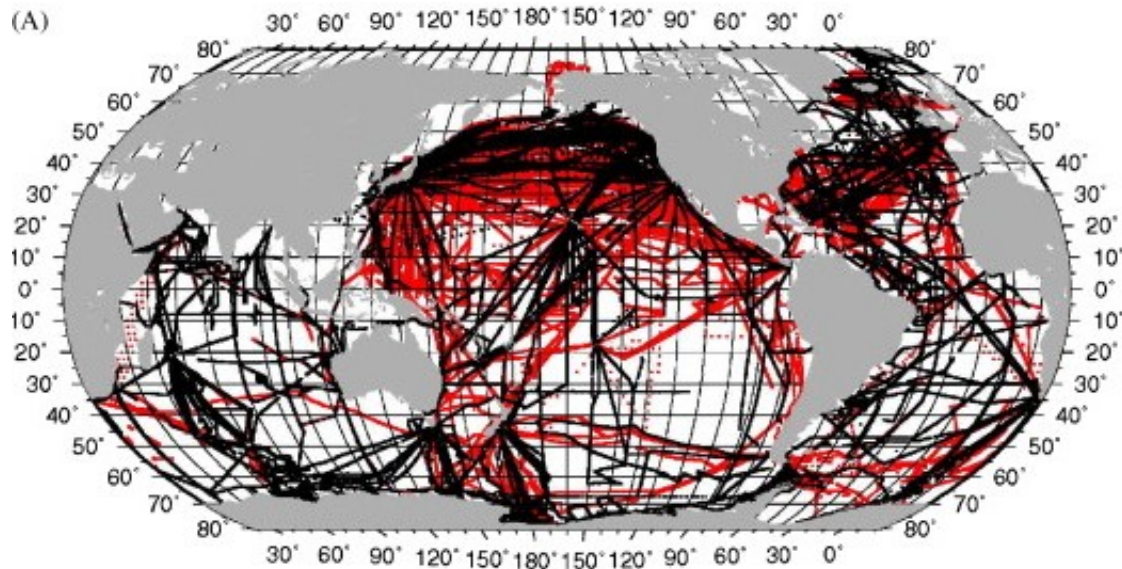
$$\mathcal{S}(pCO_2^{ocean})(x) = a(x)\mathcal{S}(SST)(x) + b(x)\mathcal{S}(Chl\_a)(x) + c(x)\mathcal{S}(pCO_{2LR}^{ocean}) + d(x)\mathcal{S}(SSS) + e(x)$$

- Extend the estimations of inferred  $pCO_2$  to regions in the interior of ocean basins where more in-situ data are available, thereby improving the validation of the method.

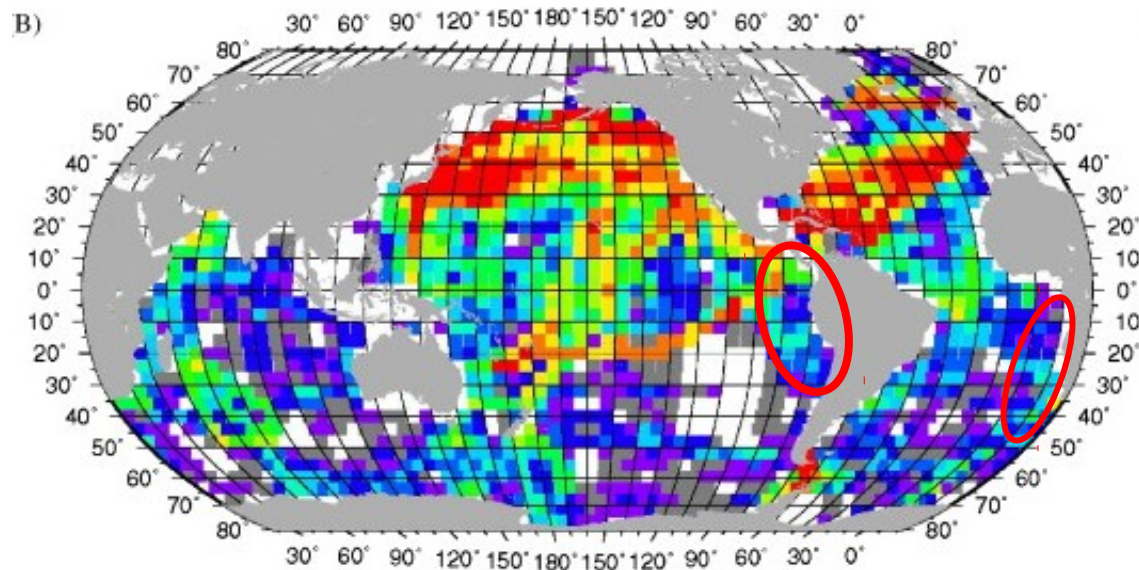


SOCAT version 2  
(2000-2010)

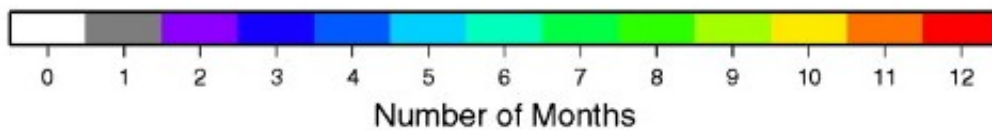
Thank you for your attention !!



**Red tracks: new data since  
Takahashi et al., 2002**



**Number of months in each  
4°x5° box with at least one  
pCO<sub>2</sub> measurement since  
early 70's**





# How to do it?

Microcanonical Multiscale Formalism: geometrical assessment of turbulent systems

## 1. How to extract the small structure information ? Singularity Exponents

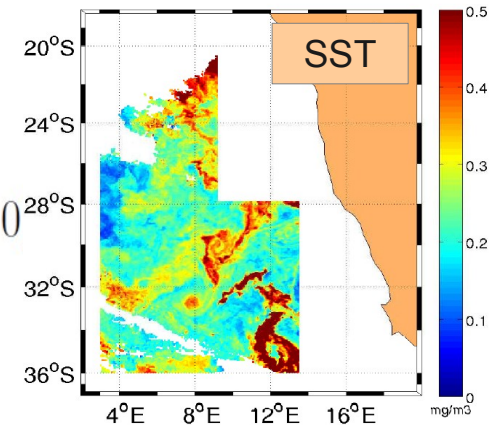
- Measure of the degree of regularity of the image, associated to transitions:  
Limiting behaviour of gradients

$$\mathbb{T}_{r,s}(x) = \int \int_{\mathcal{B}(x,r)} \|\nabla s\|(y) dy$$

- Measure of the reconstructibility of a signal: Most Singular Components,

$$\mathbb{T}_{r,s}(x) = \alpha(x)r^{h(x)+2} + o(r^{h(x)+2}) \quad (r \rightarrow 0)$$

$$\mathcal{F}_h = \{ \mathbf{x} : h(\mathbf{x}) = h \}$$

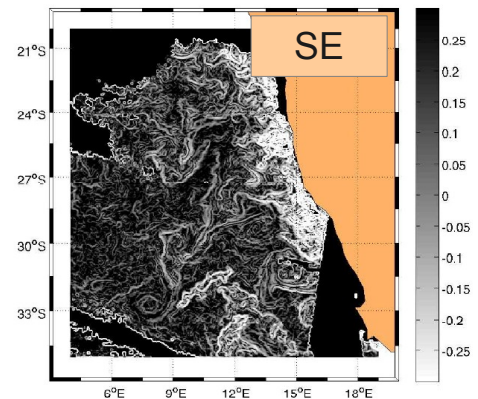


## 2. How to connect different tracer images?

- Functional dependencies :  $pCO_2 \rightleftharpoons pCO_2(SST, CHL) \longrightarrow$  Multilinear regression  
 $SE(pCO_2) = SE(pCO_2)(SE(SST), SE(CHL))$

$$SE(p_{CO_2}^{ocean})(x) = a(x)SE(SST)(x) + b(x)SE(Chl_a)(x) + c(x)SE(p_{CO_2}^{ocean}(LR)) + d(x)$$

Regression coefficients  $a(x), b(x), c(x)$  estimated from ROMS simulations data



## 3. How to propagated the information across scales?

Optimal Wavelet decomposition of the signals at different scales in order to obtain the local variable transferring information.

$$WS(p_{CO_2}^{ocean})(u, r_1) = \eta_{r_1/r_2}(x) WS(p_{CO_2}^{ocean})(u, r_2) \longrightarrow \eta_{r_1/r_2}(x) = \frac{\alpha_p(x)}{\alpha_c(x)} \longrightarrow \begin{matrix} \text{Cascade} \\ \text{coefficients} \end{matrix}$$

### 3. Cross-scale inference of pCO<sub>2</sub> data

Decomposition of the signals at different scales: Wavelet projections

Optimal Wavelets: The set of points the **Most Singular Manifold** (smallest values of h)

$$\mathcal{F}_\infty = \{\mathbf{x} : h(\mathbf{x}) = h_\infty = \min(h(\mathbf{x}))\}$$

**Most Singular Manifold:**

- Geometrical place where the transitions are the strongest.
- Associated with the highest frequencies in a turbulent signal where the multifractal hierarchy  $F_h$  converges.

➔ Multifractal hierarchy correspond to a description of the detail spaces of a multiresolution analysis performed on a turbulent signal.

$A_j$  orthogonal projection of  $V_j$  (approximation space)

$P_j$  orthogonal projection of  $W_j$  (detail space)



Reconstruction formula

$$A_{j-1}pCO_2 = A_jpCO_2 + P_jh$$

*Sudre et al. 2014*

Using reconstruction formula, the multiresolution analysis on signal  $S(pCO_2)$ (proxy) and the cross-scale inference on physical variable pCO<sub>2</sub> at low-resolution we can derive the pCO<sub>2</sub> at super-resolution of SST and Chl-a.

# Input Data

## - CarbonTracker air-sea fluxes at low resolution: 1° ~ 100 km

Temporal evolution of a tracer  $c$  in the atmosphere :

$$\frac{\partial c}{\partial t} = -u\nabla c + \frac{1}{\rho}\nabla(\rho T_d\nabla c) + \frac{1}{\rho}g + \underbrace{F}_{F, \text{ net flux at the interface}}$$

-  $F$  can be estimated using optimal control and inverse problem modeling from atmospheric  $\text{CO}_2$  data provided by SCIAMACHY and GOSAT. (Garbe et al. 2007, 2014)

- Since SCIAMACHY and GOSAT sampling is not dense enough in Benguela we use data of  $\text{CO}_2$  fluxes from CarbonTracker (Peters et al. 2007)

Relation between net air-sea flux and  $p\text{CO}_2$

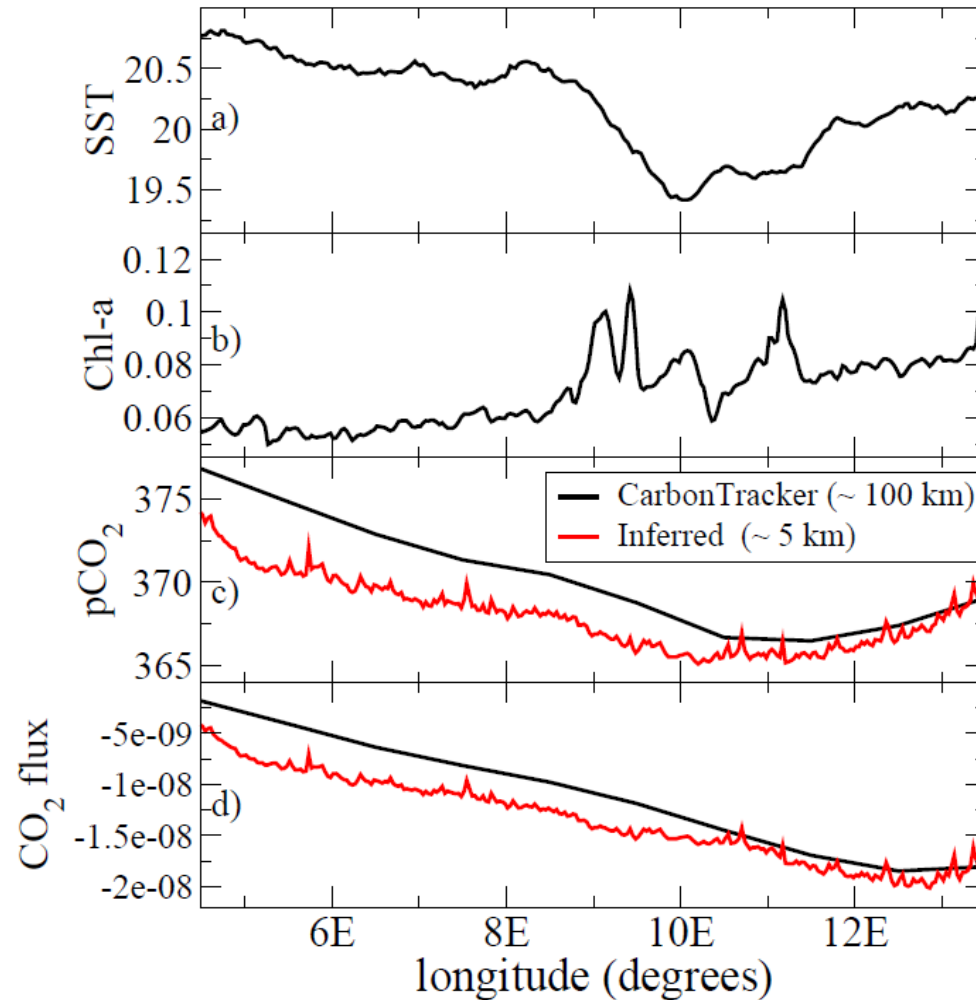
$$\underbrace{F}_{F} = \alpha K (p_{\text{CO}_2}^{\text{air}} - p_{\text{CO}_2}^{\text{ocean}})$$

- $\alpha$ , gas solubility:  $\alpha = \alpha(\text{SST}, \text{salinity})$
- $K$ , gas transfer velocity:  $K = K(\text{wind}, S, T^a, \text{sea state})$  obtained from EO data and parameterization developed by Sweeney et al. 2007.
- $p_{\text{CO}_2}^{\text{air}}$  assumed constant over the upwelling region under study (Ascension Island station)
- So  $p_{\text{CO}_2}^{\text{ocean}}$  obtained from inverse modeling and satellite data at resolution of CarbonTracker .

## - SST and Chl-a from Satellite at high resolution: ~ 4 km

Name reference	Parameter	Instruments	Satellites	Resolution
OSTIA	SST	OSTIA (Optimal interpolation)	GHRSSST	5 km / daily
MODIS	SST	MODIS	AQUA	4 km / daily
MERIS	Chl-a	MERIS	ENVISAT	4 km / daily
Globcolour	Chl-a	MODIS/MERIS/SeaWiFS (Merged globcolour)	AQUA/ENVISAT	4 km / daily

## Longitudinal profiles at 33.5°S

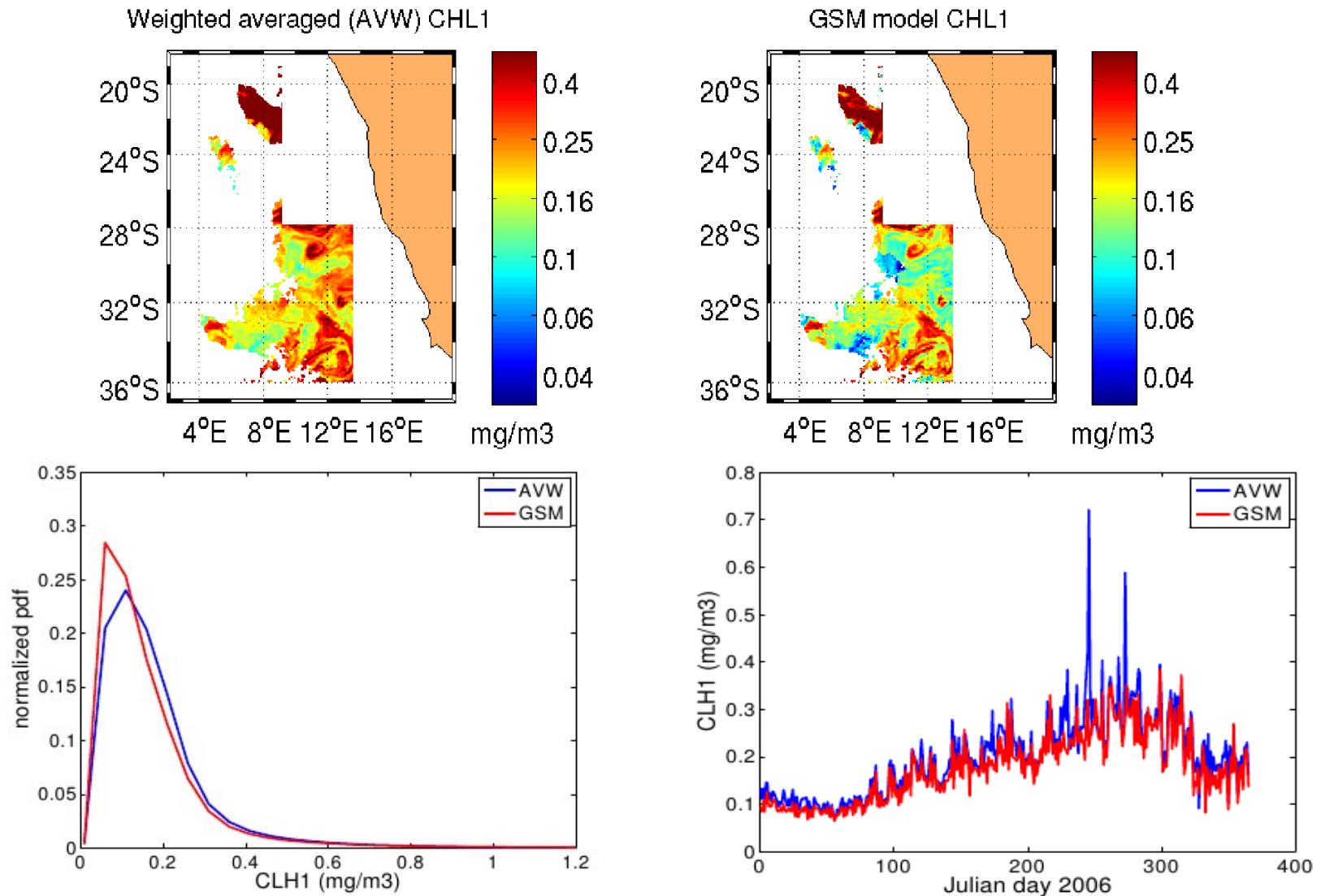


Small spatial scale variability and large spatial scale variability (different shape of profile between CarbonTracker and Inferred pCO<sub>2</sub>)

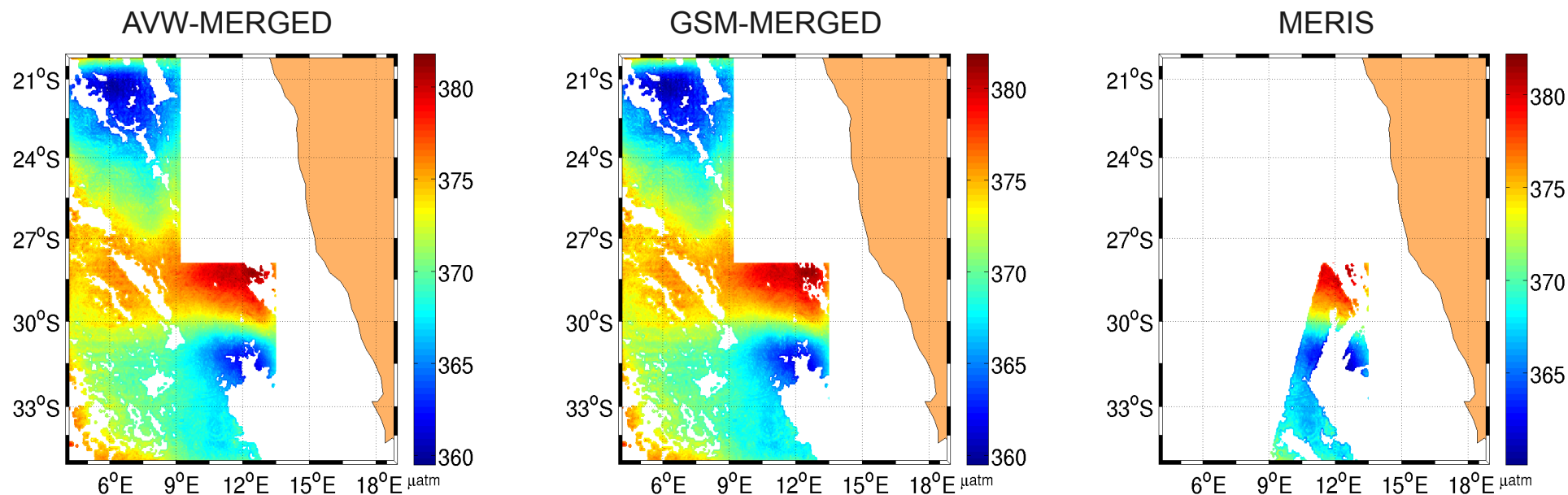
# Globcolour merged products

AVW (Weighted Average Value): Values of chl\_a are weighted by the relative error for each sensor on the simple averaging.

GSM (Garver, Siegel, Maritorena Model): fully normalized water leaving radiances



# Inferred pCO<sub>2</sub> using AVW and GSM merged products for ocean color



Comparison of number of points in the pCO<sub>2</sub> fields

Number of points in the pCO <sub>2</sub> fields			
	2006	2008	2006+2008
N° Points MERIS	4306877	5493899	<b>9800776</b>
N° Points AVW-MERGED	13500676	12881396	<b>26382072</b>
N° Points GSM-MERGED	14000396	13312647	<b>27313043</b>
Proportion AVW-MERGED/MERIS	3.14	2.34	<b>2.69</b>
Proportion GSM-MERGED/MERIS	3.25	2.42	<b>2.78</b>
Proportion AVW-MERGED/GSM-MERGED	1.03	1.03	<b>1.03</b>

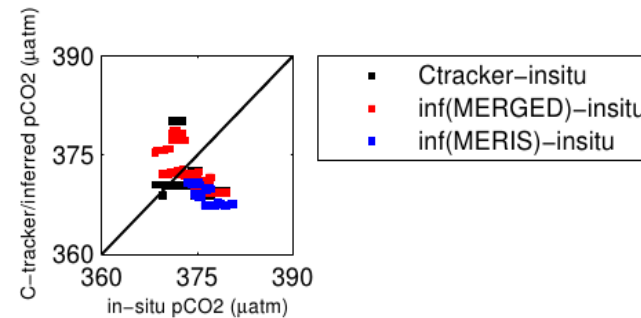
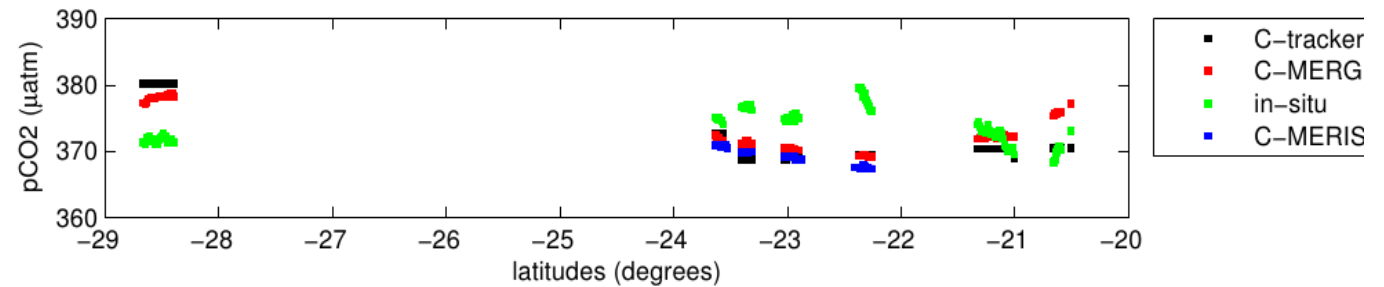
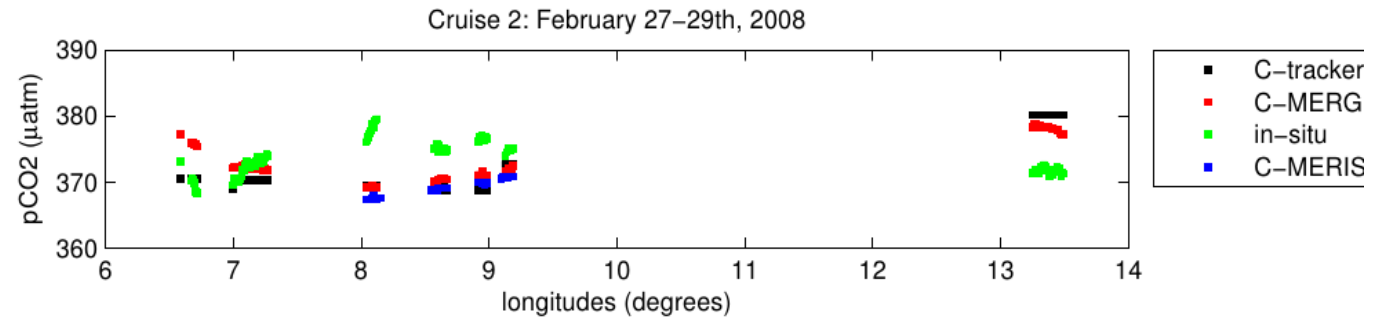
The number of points is **2.69** and **2.78** times larger when we used AVW and GSM MERGED products as compared with MERIS



# Validation of CarbonTracker and inferred super-resolution pCO<sub>2</sub> using in-situ measurements

- AVW-MERGED 2008

All intersection points

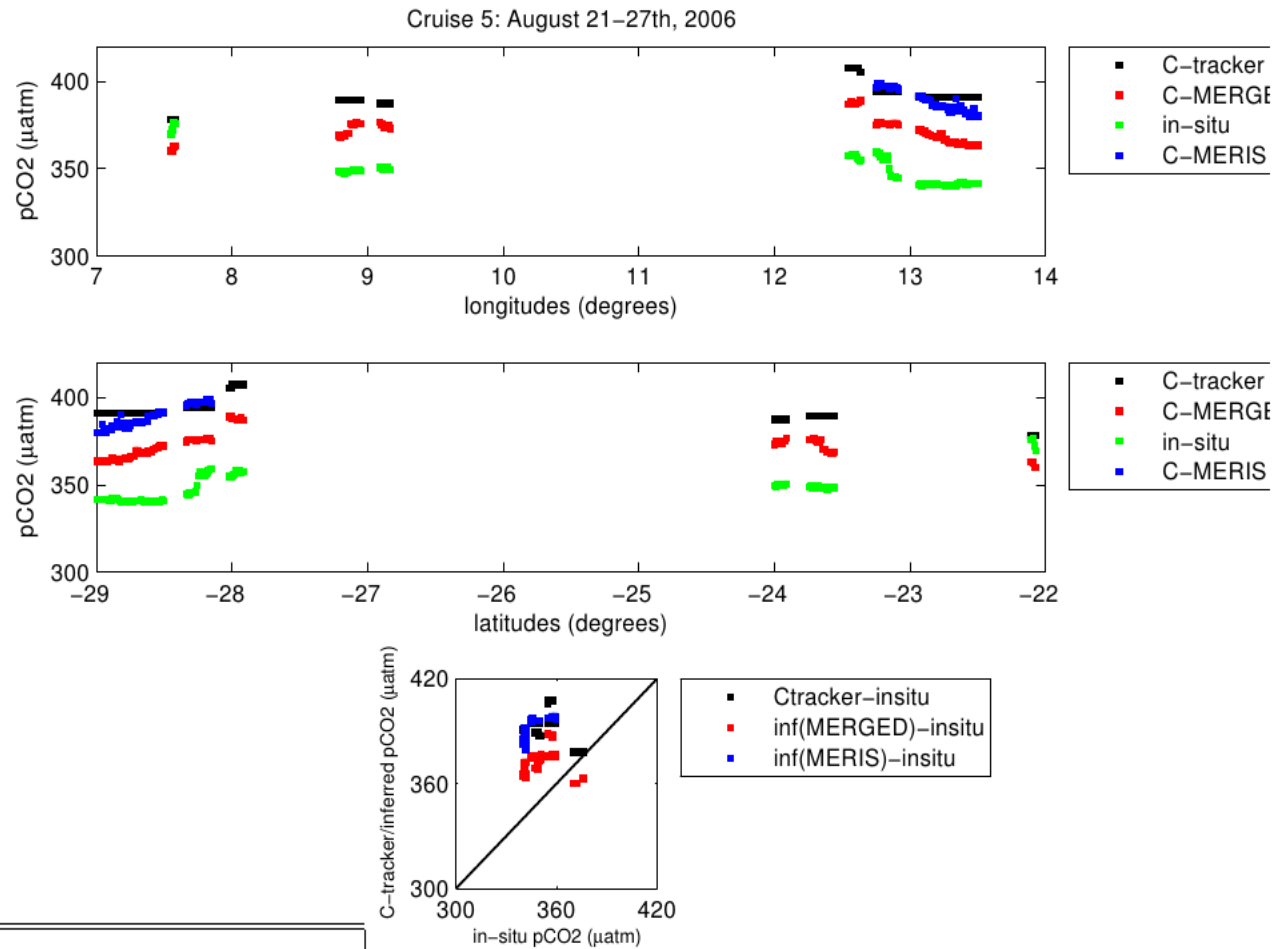


## Statistical computations

	MERIS	MERGED
N intersections	510	819
Mean Error carbontracker-insitu ( $\mu atm$ )	-3.6202	-6.2576
Mean Error inferred-insitu ( $\mu atm$ )	-6.6144	-8.2747
Mean Absolut Error carbontracker-insitu ( $\mu atm$ )	20.2404	19.9042
Mean Absolut Error inferred-insitu ( $\mu atm$ )	17.6495	18.2203
Mean Relative error carbontracker-insitu	0.0543	0.0523
Mean Relative error inferred-insitu	0.0467	0.0474

# - AVW-MERGED 2006

## All intersection points

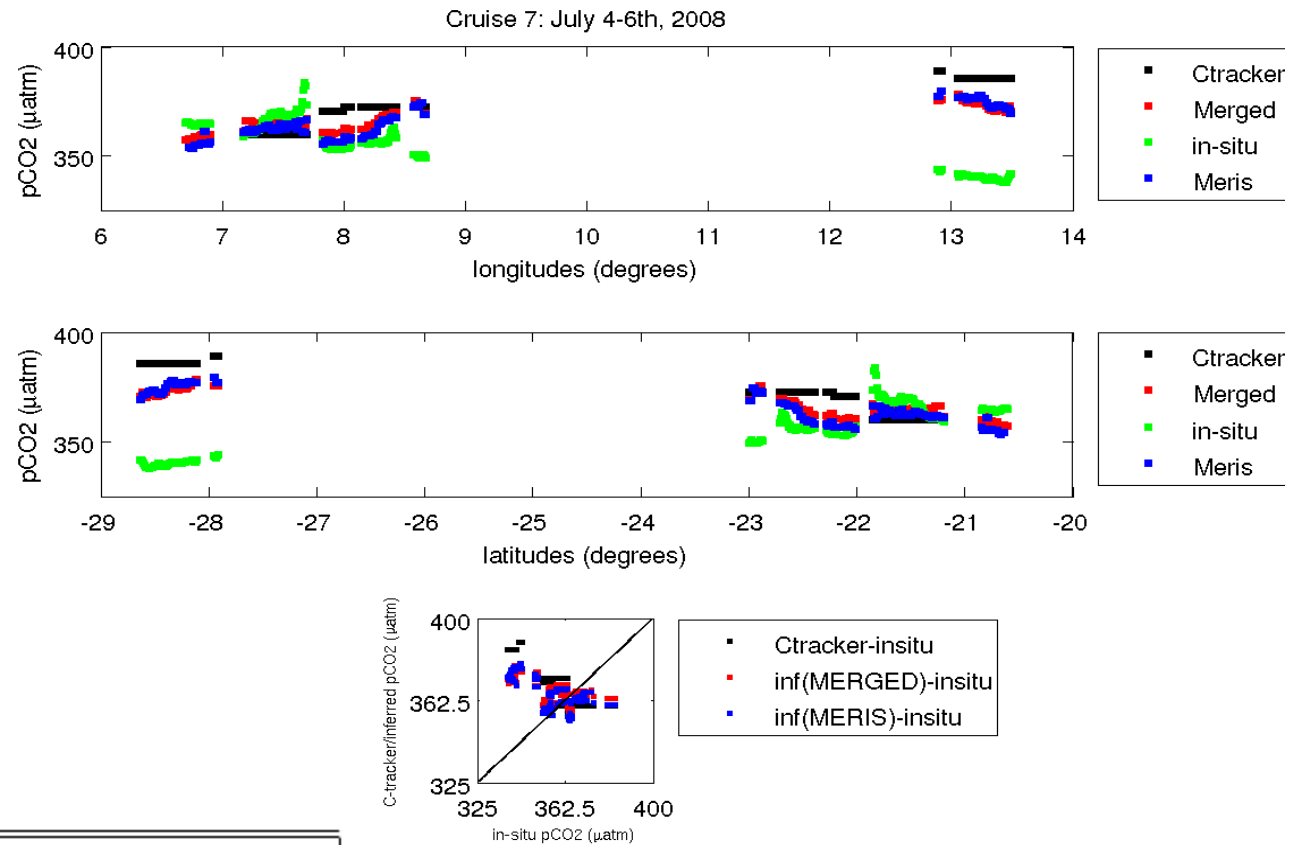


Statistical computations

	MERIS	Globcolour Merged (Weighted Average)
Number of valid intersections	237	1047
Mean Error carbontracker-insitu ( $\mu atm$ )	17.14	21.16
Mean Error inferred-insitu ( $\mu atm$ )	13.86	12.84
Mean Absolute Error carbontracker-insitu ( $\mu atm$ )	23.71	24.57
Mean Absolute Error inferred-insitu ( $\mu atm$ )	18.03	15.68
Mean Relative Error carbontracker-insitu	0.068	0.069
Mean Relative Error inferred-insitu	0.051	0.044

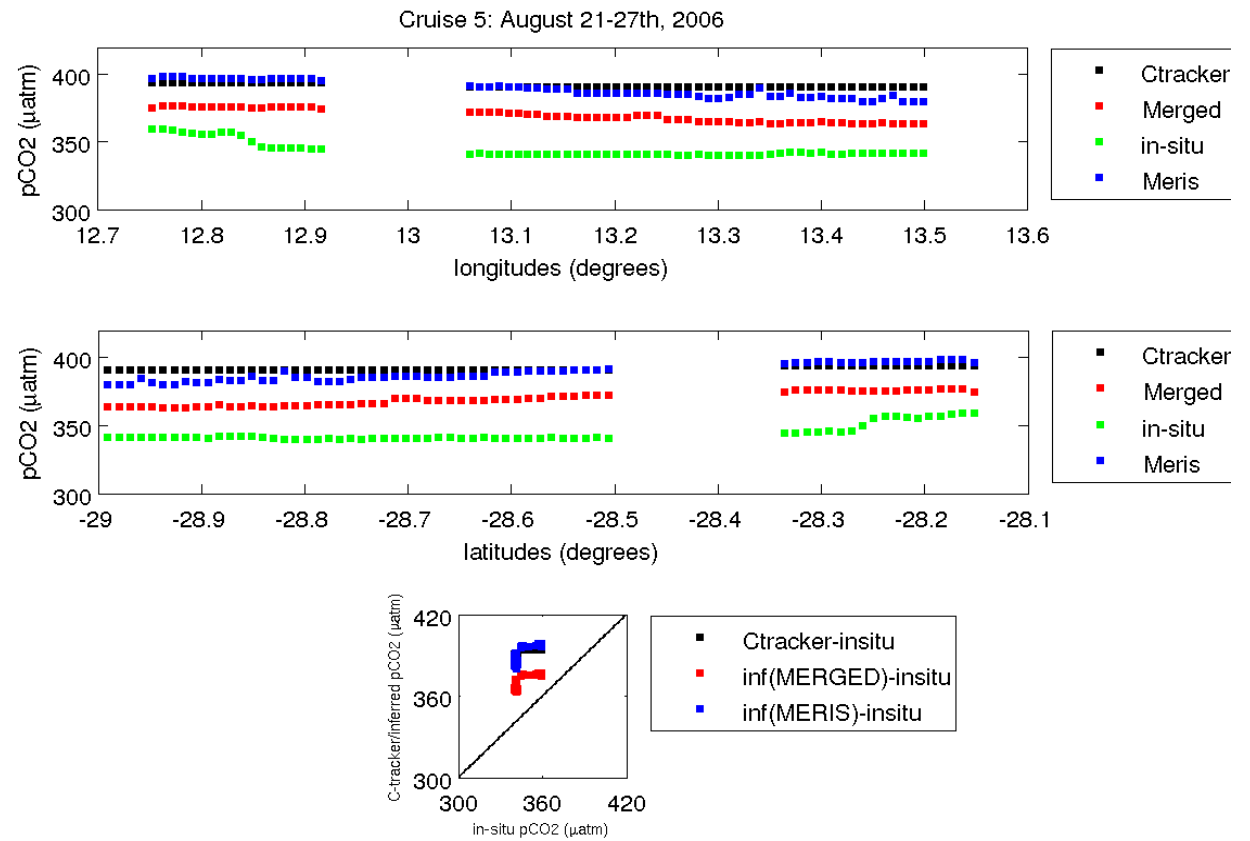
# - AVW-MERGED 2008

## At same points meris-merged



### Statistical computations

	MERIS	MERGED
N intersections	486	486
Mean Error carbontracker-insitu ( $\mu atm$ )	-3.73	-3.03
Mean Error inferred-insitu ( $\mu atm$ )	-6.62	-5.41
Mean Absolut Error carbontracker-insitu ( $\mu atm$ )	20.65	19.93
Mean Absolut Error inferred-insitu ( $\mu atm$ )	18.11	17.82
Mean Relative error carbontracker-insitu	0.055	0.053
Mean Relative error inferred-insitu	0.048	0.047



Statistical computations

	MERIS	Globcolour Merged (Weighted Average)
Number of valid intersections	236	236
Mean Error carbontracker-insitu ( $\mu atm$ )	17.14	17.21
Mean Error inferred-insitu ( $\mu atm$ )	13.86	9.64
Mean Absolute Error carbontracker-insitu ( $\mu atm$ )	23.72	23.81
Mean Absolute Error inferred-insitu ( $\mu atm$ )	18.03	13.37
Mean Relative Error carbontracker-insitu	0.068	0.068
Mean Relative Error inferred-insitu	0.0515	0.038

## Global statistics

### All intersections

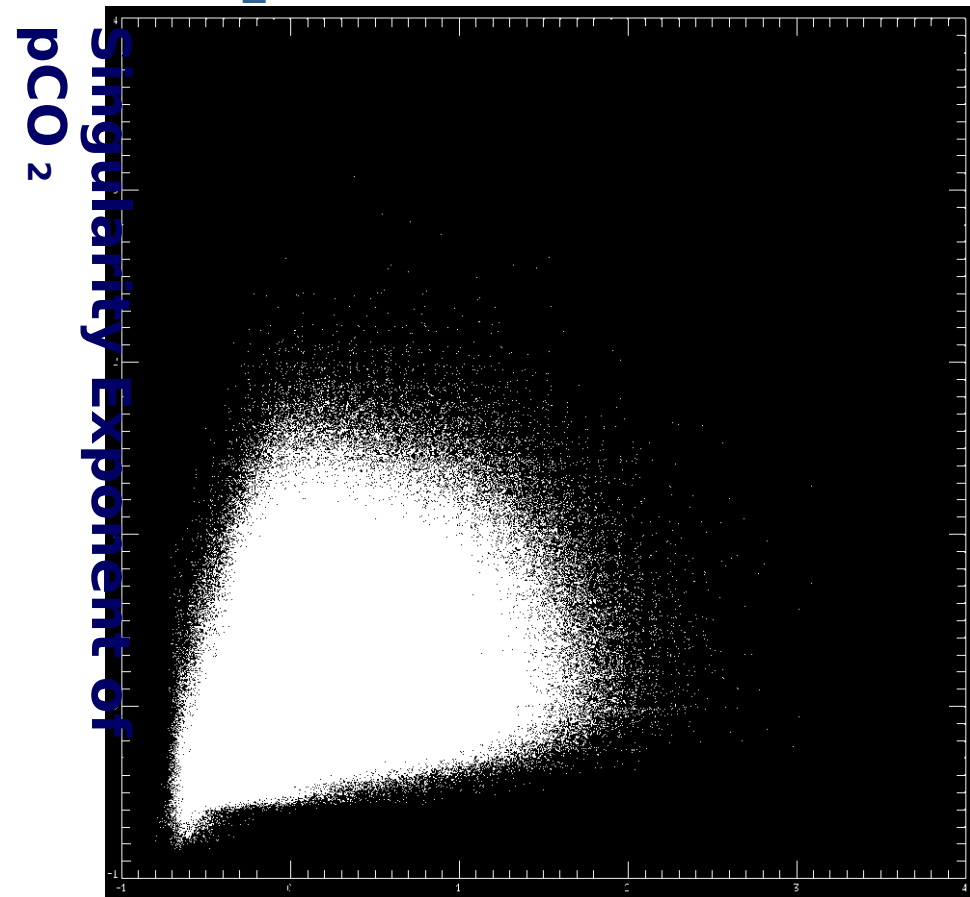
Statistical computations all cruises QUIMA2006/2008				
	MERIS	Globcolour merged (weighted average)	MERIS	Globcolour merged (GSM)
Number of valid intersections	747	1866	747	1928
Mean Error carbontracker-insitu ( $\mu atm$ )	2.97	9.12	2.97	8.83
Mean Error inferred-insitu ( $\mu atm$ )	-0.12	3.57	-0.15	3.42
Mean Absolute Error carbontracker-insitu ( $\mu atm$ )	21.34	22.52	21.34	22.08
Mean Absolute Error inferred-insitu ( $\mu atm$ )	17.77	16.79	17.77	16.47
Mean Relative Error carbontracker-insitu	0.059	0.062	0.059	0.060
Mean Relative Error inferred-insitu	0.048	0.045	0.048	0.044

### At same points meris-merged

Statistical computations all cruises QUIMA2006/2008				
	MERIS	Globcolour merged (weighted average)	MERIS	Globcolour merged (GSM)
N intersections	722	722	743	743
Mean Error carbontracker-insitu ( $\mu atm$ )	3.07	3.58	3.02	3.53
Mean Error inferred-insitu ( $\mu atm$ )	0.12	-0.49	-0.04	-0.66
Mean Absolute Error carbontracker-insitu ( $\mu atm$ )	21.67	21.20	21.52	20.88
Mean Absolute Error inferred-insitu ( $\mu atm$ )	18.08	16.36	17.91	15.54
Mean Relative Error carbontracker-insitu	0.059	0.058	0.059	0.055
Mean Relative Error inferred-insitu	0.049	0.044	0.048	0.041

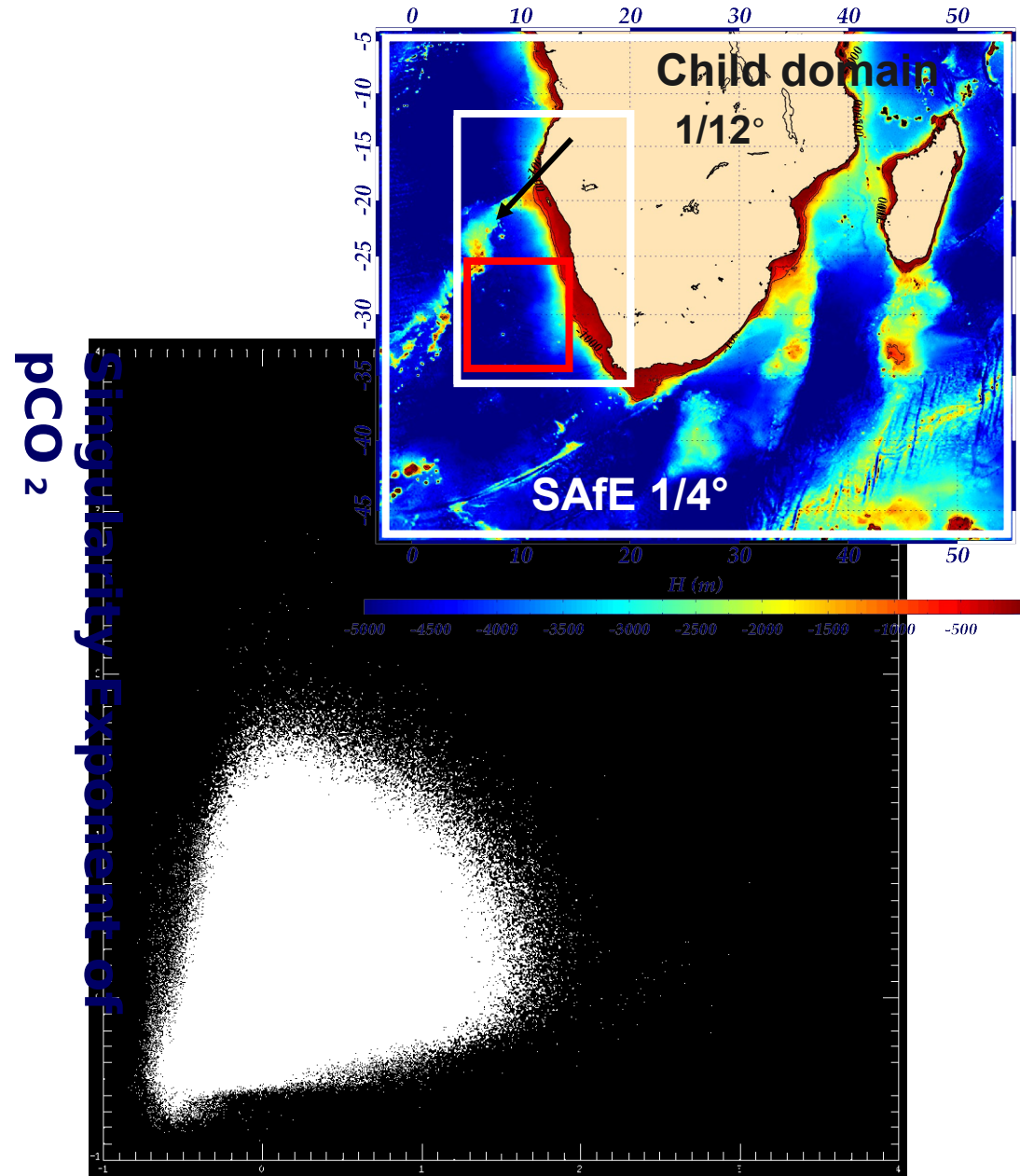
Values for merged inferred pCO<sub>2</sub> are closer to insitu measurement than MERIS inferred pCO<sub>2</sub>. GSM as a better candidate

# Properties diagrams of SE: $pCO_2$ vs SST and $pCO_2$ vs Chl-a



**Singularity Exponent of SST**

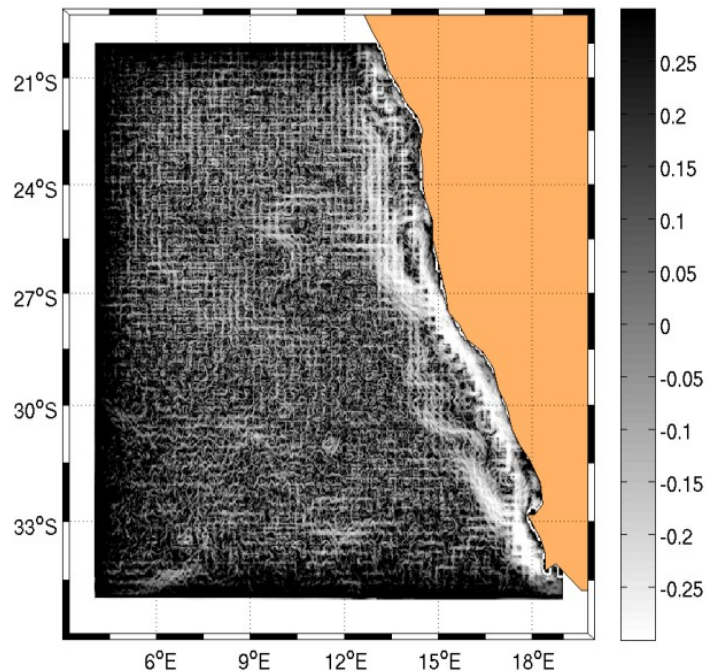
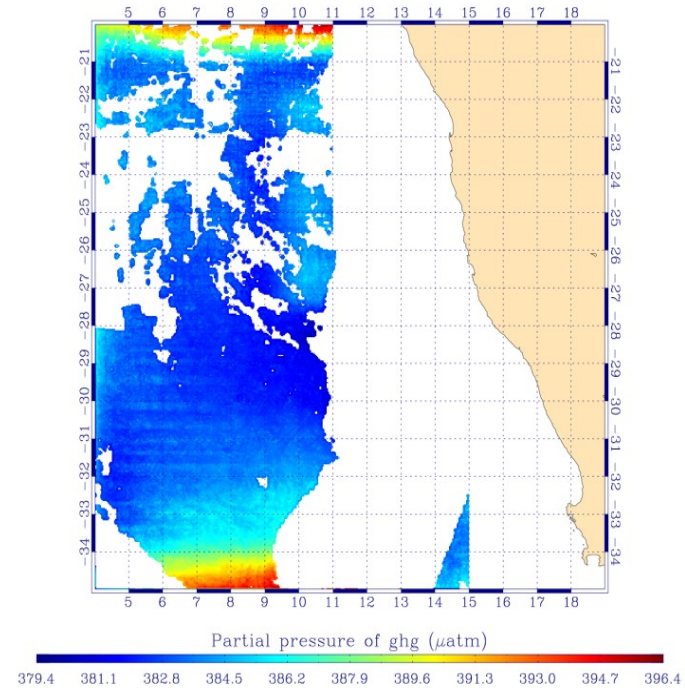
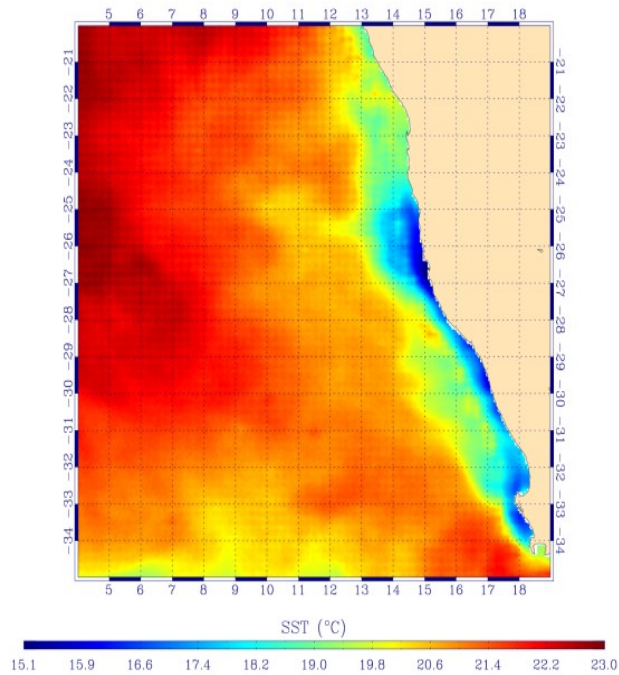
**10 years of IPSL present :  
1990-2000 with downscaled  
winds over the Benguela  
upwelling  
(Machu et al.,2014)**



**Singularity Exponent of Chl-a**



# Effect of merged OSTIA SST in the inference of superresolution pCO2



OSTIA SST introduce regular and periodic horizontal lines in the background.

Singularity exponents show clearly this grid pattern.  
Singularity exponents as a powerful tool to detect spurious patterns in data sets.